0013-7227/06/$15.00/0
Printed in U.S.A.

Endocrinology 147(9):4463–4475

doi: 10.1210/en.2005-1610

Peroxisomal Proliferator-Activated Receptor-γ Agonists Induce Partial Reversion of Epithelial-Mesenchymal Transition in Anaplastic Thyroid Cancer Cells

Aurora Aiello, Giuseppe Pandini, Francesco Frasca, Enrico Conte, Antonella Murabito, Antonella Sacco, Marco Genua, Riccardo Vigneri, and Antonino Belfiore

Dipartimento di Medicina Clinica e Sperimentale (A.A., A.M., A.S., A.B.), Cattedra di Endocrinologia, University of Catanzaro, 88100 Catanzaro, Italy; Dipartimento di Scienze Biomediche (E.C.), University of Catania, 95125 Catania, Italy; and Dipartimento di Medicina Interna e Medicine Specialistiche (G.P., F.F., M.G., R.V.), Cattedra di Endocrinologia, University of Catania, Ospedale Garibaldi, 95123 Catania, Italy

Anaplastic thyroid cancer (ATC) is an extremely aggressive tumor characterized by marked epithelial mesenchymal transition, which leads, almost invariably, to death. Peroxisomal proliferator-activated receptor (PPAR)-γ agonists have recently emerged as potential antineoplastic drugs. To establish whether ATC could be a target of PPARγ agonists, we first examined PPARγ protein expression in a panel of six ATC cell lines and then studied the biologic effects of two PPARγ agonists, ciglitazone and rosiglitazone, that belong to the class of thiazolidonediones. PPARγ protein was present and functional in all ATC cell lines. Both ciglitazone and rosiglitazone showed complex biological effects in ATC cells, including inhibition of anchorage-dependent and -independent growth and migration, and increased apoptosis rate. Rosiglitazone-induced growth inhibition was associated with cell cycle arrest and changes in cell cycle regulators, such as an increase of cyclin-dependent kinases inhibitors $p21^{cip1}$ and $p27^{kip1}$, a decrease of cyclin D1, and inactivation of Rb protein. Rosiglitazone-induced apoptosis was associated with a decrease of $Bcl\text{-}X_L$ expression and caspase-3 and -7 activation. Moreover, rosiglitazone antagonized IGF-I biological effects by up-regulating phosphatase and tensin homolog deleted from chromosome 10 with subsequent inhibition of the phosphatidylinositol 3-kinase/Akt signaling pathway. Finally, rosiglitazone increased the expression of thyroid-specific differentiation markers. In conclusions, these data suggest that PPARγ agonists induce a partial reversion of the epithelial mesenchymal transition in ATC cells by multiple mechanisms. PPARγ agonists may, therefore, have a role in the multimodal therapy currently used to slow down ATC growth and dissemination. (*Endocrinology* 147: 4463–4475, 2006)

ANAPLASTIC CANCER OF the thyroid (ATC) accounts for approximately 2–4% of thyroid carcinomas and is an extremely aggressive disease (1). Whereas 80–85% of thyroid carcinomas are well differentiated and most of them have a favorable prognosis, ATC is almost invariably fatal with a median survival ranging 4–7 months from diagnosis. Because of the relative rarity of the disease and the poor survival, the optimal therapeutic approach to ATC is uncertain. Some improvement has been reported in individual patients who have undergone multimodal therapy, including thyroidectomy, chemotherapy, and external radiation (1, 2). However, the impact of therapy on survival is poor and only very few patients survive longer than 5 yr.

Epidemiological and histopathological evidences suggest that ATC may arise from dedifferentiation of long-standing, well-differentiated thyroid tumors. Accordingly, anaplastic cancer cells have lost the ability to uptake iodine, which is a hallmark of normal thyroid follicular cells and well-differentiated thyroid carcinomas. This has therapeutical implications because radiometabolic therapy with ^{131}I is useful for residual or metastatic well-differentiated thyroid cancer but not ATC. It is clear, therefore, that new molecular targets need to be identified for an effective therapeutical strategy of ATC.

Although ATC cells originate from thyroid follicular epithelial cells, they are characterized by a mesenchymal phenotype, as revealed by spindle-shaped cells and absent or reduced levels of E-cadherin and other markers of thyroid cell differentiation [thyroglobulin, sodium-iodine symporter (NIS), thyroperoxidase, and TSH receptor (TSH-R)]. Epithelial-mesenchymal transition (3) is typical of dedifferentiated tumors and is associated with high invasion and dissemination potential (4). Typically, epithelial mesenchymal transition (EMT) is particularly pronounced in ATC.

Also the activation of the IGF system plays a role in EMT (3), and we recently observed that the IGF system is up-

First Published Online June 15, 2006

Abbreviations: ATC, Anaplastic thyroid cancer; Bax, Bcl-2-associated X protein; Bcl2, B-cell leukemia-2; CDK, cyclin-dependent kinase; EMT, epithelial mesenchymal transition; FCS, fetal calf serum; IGF-IR, IGF-I receptor; IRS, insulin receptor substrate; MTT, dimethylthiazoldiphenyltetrazoliumbromide; NIS, sodium-iodine symporter; PI, propidium iodide; PI3K, phosphatidylinositol 3-kinase; PPAR, peroxisomal proliferator-activated receptor; PPRE, peroxisome proliferator response element; PTEN, phosphatase and tensin homolog deleted from chromosome 10; Rb, retinoblastoma protein; siRNA, small interfering RNA; Smac, second mitochondrion-derived activator; Tg, thyroglobulin; TPO, thyroperoxidase; TSH-R, TSH receptor; TZD, thiazolidinedione; Z-VAD-fmk, *N*-benzyloxycarbonyl-Val-Ala-Asp-fluoromethylketone.

***Endocrinology* is published monthly by The Endocrine Society (http://www.endo-society.org), the foremost professional society serving the endocrine community.**

regulated in thyroid cancer (5, 6). In ATC this is partially due to the activation of an autocrine loop involving overexpression of the insulin receptor isoform A and enhanced autocrine production of IGF-II, which binds insulin receptor isoform A with high affinity and stimulates growth, resistance to apoptosis, and cell migration (5).

Recently agonists of peroxisomal proliferator-activated receptor (PPAR)-γ have emerged as promising tumor response modifiers. PPARγ is a ligand-activated transcription factor that belongs to the steroid receptor superfamily and is predominantly expressed in adipose cells in which it is a major inducer of differentiation and adipogenesis (7). Specific ligands to this factor have been identified such as the prostanoid 15d-PGJ2 and the antidiabetic agents thiazolidinediones (TZDs) (8). PPARγ agonists induce a variety of favorable changes (growth arrest, apoptosis, and/or partial redifferentiation) in certain malignancies, including liposarcoma and cancers of the breast, colon, pancreas, and prostate (9–17). Interestingly recent studies have shown the presence of a paired box gene 8-PPARγ rearrangement in a subgroup of follicular thyroid cancers. The resulting fusion protein inhibits PPARγ activation in a dominant-negative manner and has an oncogenic role (18). Moreover, it has been recently shown that PPARγ insufficiency promotes thyroid carcinogenesis in mice harboring a knockin mutant thyroid hormone β-receptor, which spontaneously develop follicular thyroid carcinomas (19).

These studies may suggest, therefore, an antioncogenic role of PPARγ in the thyroid. Moreover, PPARγ forms heterodimers with the retinoid X receptor. PPARγ agonists may therefore synergize with retinoids, such as all-trans retinoic acid, which induces growth arrest and partial redifferentiation in various cancer cells, including poorly differentiated thyroid cancer cells (20). Phase II studies using 13-*cis*-retinoic acid in patients with poorly differentiated thyroid cancer have shown induction of a partial redifferentiation in approximately 40% of cases (21).

To establish whether PPARγ agonists might be a useful adjuvant treatment in ATC, we first examined the expression of PPARγ protein in six ATC cell lines and also studied the biologic effects of two PPARγ agonists, ciglitazone and rosiglitazone, both belonging to the class of antidiabetic agents TZDs. We used rosiglitazone at doses comparable with those reached during diabetes therapy. We found that both these TZDs have complex biological effects in ATC cells, including reduction of anchorage-dependent and -independent growth and migration, and increased apoptosis rate. Moreover, rosiglitazone antagonized, at least in part, the biological effects of IGF-I by up-regulating phosphatase and tensin homolog deleted from chromosome 10 (PTEN) and consequently inhibiting the phosphatidylinositol 3-kinase (PI3K)/Akt signaling pathway. It also potentiated the antitumor effect of doxorubicin and induced a partial redifferentiation in ATC cells.

Taken together, these effects confirm the antitumor potential of these agents in ATC cells, with a partial reversion of EMT. These observations suggest a possible role of PPARγ agonists in the multimodal therapy for ATC.

Materials and Methods

The following materials were purchased: fetal calf serum (FCS), culture media, BSA, glutamine, bacitracin, vanadate, phenylmethylsulfonyl fluoride, monoclonal anti-β-actin antibody from Sigma (St. Louis, MO); IGF-I was purchased from Calbiochem (San Diego, CA); Fugene 6 transfection reagent was obtained from Roche Diagnostics (Mannheim, Germany); luciferase assay system was obtained from Promega Corp. (Madison, WI). Anti-PPARγ antibody (PA3–821) was obtained by Affinity Bioreagents (Deerfield, IL), and anti-PTEN antibody was obtained by Santa Cruz Biotechnology (Santa Cruz, CA). Antiphospho antibodies to Ser473 and Thr308 of Akt were from Cell Signaling (Beverly, MA). Rosiglitazone was kindly provided by Glaxo Smith Kline (Greenville, NC). Ciglitazone was purchased by Alexis Biochemicals (Lausen, Switzerland). The firefly luciferase vector driven by the PPARγ-sensitive peroxisome proliferator response element (PPRE)-3 sequences, mouse mammary tumor virus, was kindly provided by R. Evans (Salk Institute, La Jolla, CA).

Cells

Human ATC cells (FF-1, ARO, HTh74, C643, SW1736, 8305c) and human papillary cancer cells (TPC-1 and NPA) were studied. FF-1 cell line was established in our laboratory as follows. A surgical specimen from an anaplastic thyroid cancer was initially fragmented with a scalpel and subsequently digested for 1 h in DMEM low glucose (Sigma) containing 1 mg/ml type V collagenase (Sigma) in a 37 C water bath with agitation. The cell suspension was then centrifuged and the pellet resuspended in complete RPMI 1640. Cells were then subsequently cultured with RPMI 1640 containing increasing doses (from 1 to 10%) of stripped FCS containing 100 μg/ml penicillin and streptomycin and 2 mM glutamine. Cultures were analyzed by immunofluorescence using an antibody against cytokeratin (Novocastra Laboratories, Newcastle Upon Tyne, UK) that stains exclusively epithelial cells.

ARO and TPC-1 were obtained from Drs. A. Fusco and M. Santoro (Università Federico II, Naples, Italy) and grown in RPMI 1640 (Sigma). HTh74, C643, and SW1736 cells were provided by Dr. N. E. Heldin (Uppsala University Hospital, Uppsala, Sweden), and 8305c cells were purchased from ECACC (Salisbury, UK): these cells were grown in MEM. All media were supplemented with 2 mM glutamine, 10% fetal bovine serum, and 100 μg/ml penicillin and streptomycin.

Viability assay

Cell viability was measured by the dimethylthiazoldiphenyltetrazoliumbromide (MTT) test: cells (2×10^3/well) were seeded in 96-well plates in 10% FCS-containing medium. After 24 h the medium was removed and replaced with FCS-free medium containing BSA 0.1%. After an additional 24 h, either ciglitazone or rosiglitazone was added at the indicated doses. Parallel experiments were carried out in cells maintained in medium containing 10% FCS. To evaluate whether rosiglitazone affected cell viability regulation by IGF-I, serum-starved cells, incubated in the presence or absence of 10 μM rosiglitazone, were stimulated with 10 nM IGF-I. Cell viability was measured 5 d later by measuring the rate of tetrazolium salts reduction to formazan (MTT, Amersham Life Science, Buckinghamshire, UK), which is proportional to the number of living cells (22). At the end of incubation, the absorbance was read at 540 nm.

Cell growth studies

Cell growth was measured by [^{3}H]thymidine incorporation: cells (3×10^4/well) were plated in 24-well tissue culture plates and grown in their regular medium for 24 h. The medium was then replaced with fresh medium containing 0.1% BSA. Twenty-four hours later, either ciglitazone or rosiglitazone at the indicated doses was added. In parallel experiments the growth effect of 10 nM IGF-I was assessed in the presence or absence of each PPARγ agonist. After 24 h, 18.5 kBq/well of [^{3}H]thymidine were added for 4 h. Cell monolayers were then washed twice with cold buffer, incubated with cold 10% trichloroacetic acid solution for 30 min, solubilized with 0.1 N NaOH, and counted by liquid scintillation in a β-counter.

Migration assay

Cell migration was measured with the Boyden's chamber technique. Cells (10^5/well), resuspended in 200 μl medium, were placed on 6.5-mm-diameter polycarbonate filters (8 μm pore size; Corning Costar Corp., Cambridge, MA) containing polycarbonate membranes coated at the lower side with 250 μg/ml collagen IV. Cells were incubated in the presence or absence of 10 μM rosiglitazone and allowed to migrate to the underside of the top chamber for 18 h. IGF-I (10 nM) was added to the lower chamber as chemoattractant.

At the end of incubation, the cells at the upper side of the filter were removed with a cotton swab. Cells that had migrated to the lower side of the filter were fixed with 11% gluteraldeyde for 15 min at room temperature and stained with 0.1% crystal violet in 20% methanol for 20′. After three washes with water and complete drying, the crystal violet was solubilized by immersion of the filters in 10% acetic acid. The concentration of the solubilized crystal violet was evaluated as absorbance at 590 nm. Cell migration was expressed as percent of migrated cells over untreated controls.

Cell cycle and apoptosis evaluation

Cells were cultured in the absence or presence of rosiglitazone and synchronized by culturing them for 24 h in leucine-deprived medium, which induces a block at the G_1 restriction point. Cells were then released from the cell cycle block by the addition of regular medium and harvested at 12 h from release. Permeabilized cells were centrifuged and resuspended in PBS containing 20 mg/ml propidium iodide (PI) plus 40 mg/ml RNase (Sigma) for 30 min in the dark. Cells were then subjected to fluorescence-activated cell sorter analysis (Coulter Elite flow cytometer, Beckman Coulter, Milan, Italy) and gated for PI. Sub-G_1 cells were scored as apoptotic.

For annexin staining, cells were washed twice with cold PBS and then resuspended in 1 × binding buffer at a concentration of 1×10^6 cells/ml. Cells (1×10^5 cells) were then transferred to a 5-ml tube and incubated with 5 μl annexin V-fluorescein isothiocyanate and 10 μl PI for 15 min at room temperature (20–25 C) in the dark. After the addition of 400 μl of 1 × binding buffer to each tube, annexin-positive cells were scored under a fluorescence microscope. Values obtained were expressed as percent of annexin-positive cells over the total scored cell population.

Apoptosis was also determined with the cell death detection ELISA PLUS kit (Roche Diagnostics), a photometric enzyme immunoassay for the qualitative and quantitative *in vitro* determination of cytoplasmic histone-associated DNA fragments after induced cell death. Briefly, cells (2×10^4/well) were plated in 12-well tissue culture plates and grown in their regular medium for 24 h. The medium was then replaced with fresh medium containing either 20 μM ciglitazone or 10 μM rosiglitazone for 48 h. At the end of incubation, the absorbance was read at 405 nm.

Assay for caspase-3/7 activity

Caspase-3/7 activity was measured by Apo-ONE homogeneous caspase-3/7 assay (Promega), according to the manufacturer's instructions. Briefly, 9×10^4 cells were seeded in 35-mm dishes and incubated in the presence or absence of 10 μM rosiglitazone for 48 h. For the assay, 30 μl of solubilized 2×10^5 cells/ml were added to a 96-well plate and incubated with caspase-3/7 Z-DEVD-R110 substrate. The increase of fluorescence was measured every hour in a 8-h period using a spectrofluorimeter Wallac 1420 VICTOR (PerkinElmer, Boston, MA), with an excitation wavelength of 485 nm and an emission wavelength of 535 nm. The assay was carried out in the presence or absence of the caspase inhibitor *N*-benzyloxycarbonyl-Val-Ala-Asp-fluoromethylketone (Z-VAD-fmk) at the concentration of 30 μM.

Western blot analysis

Cells were grown to 70% confluency and then incubated in the presence or absence of 10 μM rosiglitazone for 48 h. For phospho-Akt analysis, cells were stimulated with 10 nM IGF-I for 10 min. At the end of the incubation, cells were washed with ice-cold PBS and lysed in Laemli buffer containing 62.5 mM Tris-HCl (pH 6.8), 2% sodium dodecyl sulfate, and 9.9% glycerol. Protein concentration was determined by BCA protein assay kit (Pierce, Rockford, IL). For analysis of other proteins, cells were lysed in cold radioimmunoprecipitation assay buffer containing 50 mM Tris (pH 7.4), 150 mM NaCl, 1% Triton X-100, 0.25% sodium deoxycolate, 10 mM sodium pyrophosphate, 1 mM NaF, 1 mM sodium orthovanadate, 2 mM phenylmethylsulfonyl fluoride, 10 μg/ml aprotinin, 10 μg/ml pepstatin, and 10 μg/ml leupeptin. After collection, samples were rotated for 15 min at 4 C. Insoluble material was separated from the soluble extract by centrifugation at 10,000 × *g* for 10 min at 4 C. Protein concentration was determined by the Bradford assay. Cell lysates were subjected to SDS-PAGE. The resolved proteins were transferred to nitrocellulose membranes and immunoblotted using 1 μg/ml of the indicated antibodies. All immunoblots were analyzed by enhanced chemiluminescence (Amersham, Little Chalfont, UK), autoradiographed, and subjected to densitometric analysis. When appropriate, the nitrocellulose membranes were stripped with buffer Restore (Pierce) for 15 min at room temperature and subsequently reprobed with an anti-β-actin mouse monoclonal antibody. Densitometric results were corrected for protein loading by normalization for β-actin expression.

Transient transfection and luciferase assays

To evaluate whether PPARγ expressed by ATC cells was functional, cells were transiently transfected with 0.3 μg of a firefly luciferase vector driven by the PPARγ-sensitive PPRE3 sequences (PPRE3-tk-luc) (23). Briefly, 2.5×10^4 cells were seeded in 12-well plates and grown for 24 h in complete medium. Transfection was carried out by adding a mixture containing 1 μg DNA and 4 μl Fugene6 in 40 μl of serum-free medium to each well. To normalize values for transfection efficiency, cells were cotransfected with 0.5 μg of a vector coding for the Renilla luciferase. Immediately after transfection, cells were treated with rosiglitazone (10 μM) and recovered 48 h later. Cell extracts and luciferase reagents were prepared with the dual-luciferase reporter assay system (Promega). Both firefly and renilla luciferase activities were then evaluated by a luminometer (Turner 20/20; Turner Industries, Sunnyvale, CA). Normalized reporter activity was calculated as the ratio of firefly luciferase values divided by the renilla luciferase values. Relative fold activation was calculated by dividing normalized values of treated cells by normalized values of control cells.

Gene silencing by small interfering RNA (siRNA)

Cells were plated onto 6-well plates (10^5/well), maintained in antibiotic-free medium for 24 h, and transfected with a mixture containing Opti-MEM, 8 μl/well LipofectAMINE 2000 (Invitrogen, San Diego, CA), and either 0.5 μg/well scramble siRNA or a mixture of four PPARγ siRNA (smart pool; Dharmacon Research, Inc., Lafayette, CO) for 5 h. The sequence of these siRNAs is available from the manufacturer. Cells were then incubated with fresh medium for 48 h until processing.

Real-time PCR

Oligo 6.3 primer analysis software (Molecular Biology Insights, Inc., West Cascade, CO) was used to design appropriate following primer pairs: 5′-TCA GGA AGG CAC TGC TTA TGG-3′ (forward) and 5′-GCC CTC TCT GGG CTG ATA ATT-3′ (reverse) specific for the human thyroglobulin (Tg); 5′-ACC TGC TCC TCA TCG CCT CT-3′ (forward) and 5′-CAA AGG AAG CAG GGC GAC AA-3′ (reverse) specific for the human TSH-R; 5′-GGC GTC GCT CCT GTC CAC-3′ (forward) and 5′-CGC CCA CAA GCA TGA CAC-3′ (reverse) specific for the human NIS; 5′-CTG CGG GAC GGT GAC T-3′ (forward) and 5′-CGC GCC TCC CAG ACT-3′ (reverse) specific for the human thyroperoxidase (TPO); primer pairs were synthesized by MWG-Biotech (Ebersberg, Germany). Total RNA (5 μg) was reverse transcribed by ThermoScript RT (Invitrogen) and Oligo dT primers. Synthesized cDNA (0.15 μl) was then combined in a PCR using 0.2 μM of specific primers.

ELE-1 (housekeeping gene) amplification was performed using the following primers: 5′-ATT-GAA-GAA-ATT-GCA-GGC-TC-3′ (forward) and 5′-TGG-AGA-AGA-GGA-GCT-GTA-TCT-3′ (reverse) (fragment size, 280 bp). Quantitative real-time PCR was performed on an ABI Prism 7700 (PE Applied Biosystems, Foster City, CA) using Sybr Green PCR master mix (PE Applied Biosystems) following the manufacturer's instructions. Amplification reactions were checked for the presence of nonspecific products by agarose gel electrophoresis. Relative quantita-

tive determination (PE Applied Biosystems user bulletin no. 2) of target gene levels was performed by ΔCt values, as previously described (24).

Results

ATC cells express functional PPARγ protein

PPARγ protein expression was measured by Western blot in six ATC cell lines and two papillary cancer cell lines. PPARγ protein was identified at variable levels at the expected molecular mass of 54 kDa in all cell lines examined except NPA papillary thyroid cancer cells (Fig. 1A). The highest PPARγ levels were observed in FF-1 and ARO ATC cells. To evaluate whether PPARγ expressed by ATC cells was functional, each ATC cell line was transfected with a PPRE3-tk-luciferase reporter and then exposed to the PPARγ agonist rosiglitazone (10 μM) for 24 h. Rosiglitazone treatment determined a significant luciferase increase (ranging from 150 to 450%) in all cell lines except NPA, demonstrating that PPARγ protein was functional in all ATC cell lines (Fig. 1B).

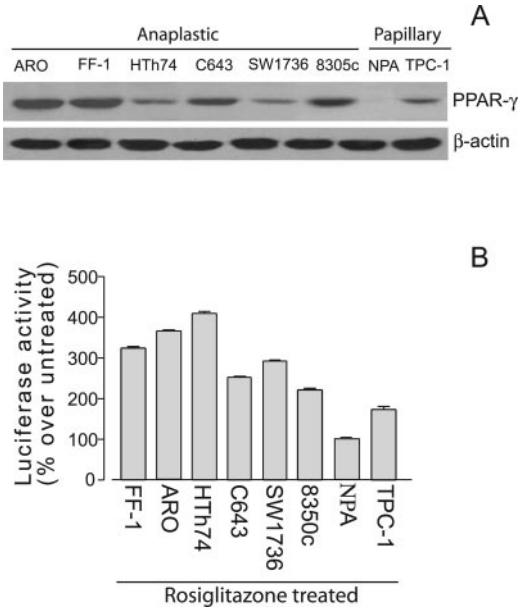

FIG. 1. PPARγ protein expression and function in ATC cells. A, PPARγ protein expression levels in thyroid cancer cells: six anaplastic cancer cell lines (FF-1, ARO, HTh74, C643, SW1736, and 8305c) and two papillary cancer cell lines (NPA and TPC-1) in monolayer culture were lysed, subjected to SDS-PAGE, and PPARγ protein expression then measured by Western blot analysis (*upper panel*) as described in *Materials and Methods*. Filters were reblotted with an anti-β-actin antibody (*lower panel*) to normalize for protein loading. The experiment shown is representative of three independent experiments. B, Rosiglitazone-induced PPARγ promoter activation. ATC cells were cotransfected with both a PPRE3-tyrosine kinase-luciferase reporter and the pRL-SV40 (Renilla luciferase expression vector) and then exposed to 10 μM rosiglitazone for 24 h. Both firefly and renilla luciferase activities were then evaluated by a Turner 20/20 luminometer. Normalized luciferase activity was calculated as the ratio of firefly luciferase values divided by the renilla luciferase values. Relative fold activation percent was calculated by first dividing normalized values of treated cells by normalized values of control cells and considering the latter as 100%.

PPARγ agonists reduce cell viability of ATC cells

The effect of two PPARγ agonists, ciglitazone and rosiglitazone, on cell viability was assessed by MTT assay. Dose-response experiments with both compounds were carried out in FF-1 and ARO cell lines. Cells were cultured in monolayers in serum containing medium and MTT staining was evaluated after a 5-d exposure to increasing doses of each PPARγ agonist. As shown in Fig. 2A, both PPARγ agonists markedly reduced cell viability, with rosiglitazone being more potent than ciglitazone. Both compounds were more effective in serum-free conditions than serum-containing medium (not shown). In FF-1 cells, viability was reduced to 50% at 16 μM rosiglitazone in serum-free medium and at 34 μM in the presence of serum. Corresponding values for ciglitazone were 44 and 64 μM (not shown). Dose-response experiments were then carried out with rosiglitazone in the remaining ATC cell lines (Fig. 2A). In all cell lines cell viability was effectively reduced by incubation with rosiglitazone, starting at 0.1–1.0 μM. In contrast, cell viability of PPARγ-negative NPA cells was unaffected by rosiglitazone at doses up to 100 μM (not shown). The effect of rosiglitazone was markedly inhibited when PPARγ was knocked down by transfection with specific siRNA cells (Fig. 2B).

Cell viability in response to both PPARγ agonists was then evaluated in all ATC cell lines using 10 μM rosiglitazone and 20 μM ciglitazone. Both PPARγ agonists reduced ATC cell viability to 44–72% of untreated cells in serum-free conditions (Table 1). Also in these conditions, PPARγ agonists were ineffective on NPA papillary cell line. To further evaluate whether this reduction of cell viability was due to PPARγ agonist binding to PPARγ, we used GW9662, a selective and high-affinity PPARγ antagonist, which covalently modifies a cysteine residue in the ligand binding site of PPARγ. Preincubation (6 h) with 1 μM GW9662 fully inhibited the effect of 10 μM rosiglitazone or 20 μg ciglitazone on cell viability (Table 1). Taken together, these data indicate that both rosiglitazone and ciglitazone affect cell viability through a PPARγ-dependent mechanism.

Because retinoids have been reported to induce growth arrest and synergize PPARγ agonist effects in a variety of tumor cells, we evaluated whether 9-*cis*-retinoic acid, at a dose of 1 μM, affected ATC cell viability. Under the conditions used, *cis*-retinoic acid slightly reduced cell viability only in ARO and FF-1 cells, whereas it was ineffective in the remaining four cell lines (Table 1). 9-*cis*-retinoic acid did not increase the effect of PPARγ agonists when used in combination (data not shown).

We next investigated whether rosiglitazone was able to potentiate the antitumor effect of doxorubicin, the chemotherapeutic agent most frequently used in ATC treatment. Cells were cultured in serum containing medium and incubated with graded doses of doxorubicin for 5 d. Under these conditions, dose-response experiments showed that a dose of doxorubicin of 0.0250 μM was able to reduce cell survival by 15–60% in all cell lines except HTh74 cells, in which the same effect was achieved with 0.0125 μM doxorubicin (data not shown). A dose of doxorubicin of 0.0125 μM. was therefore used for HTh74 cells and a dose of 0.0250 μM for all the other cell lines in combination experiments with rosiglitazone. The

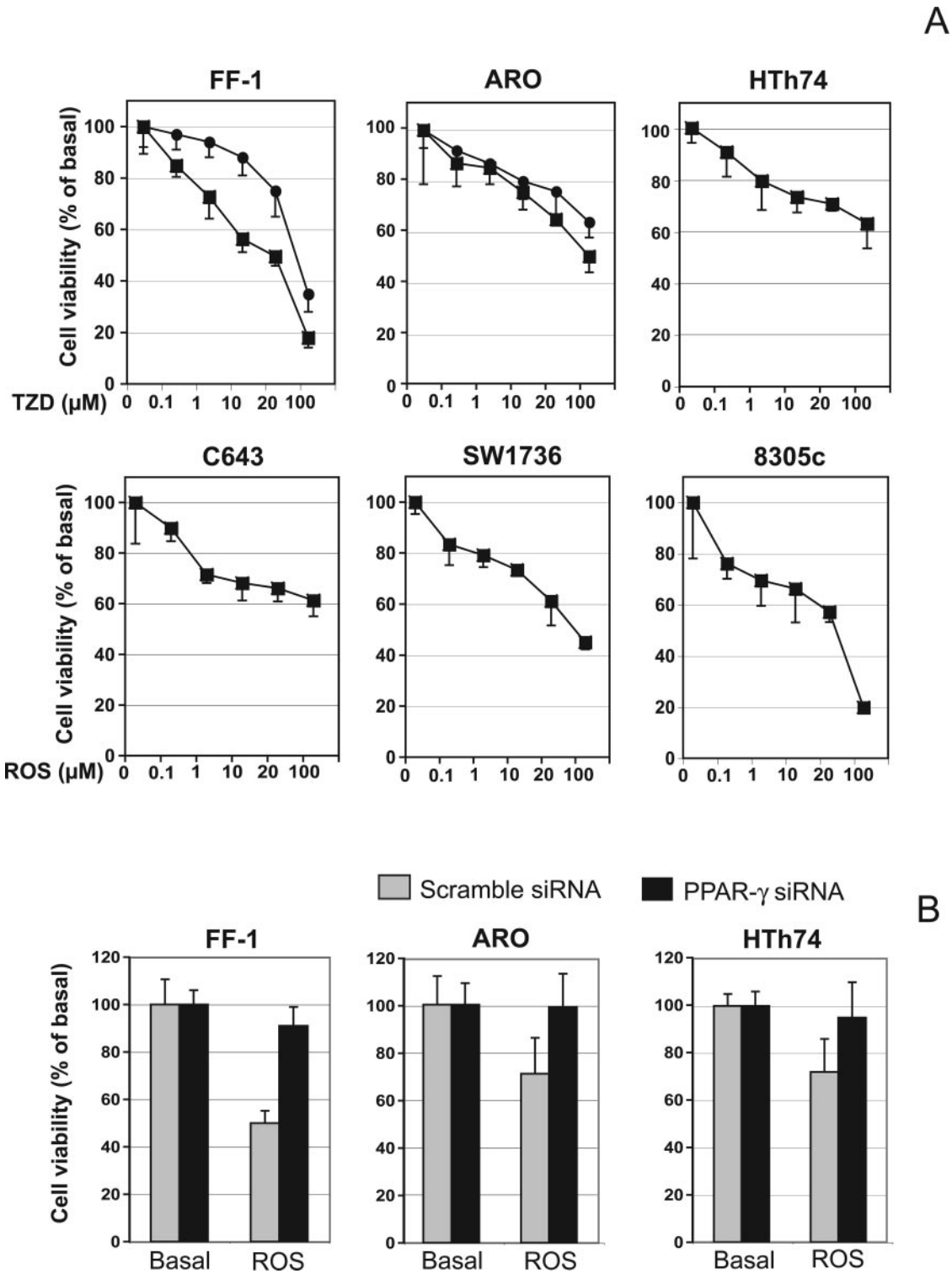

FIG. 2. Cell viability inhibition by PPARγ agonists in ATC cells. A, FF-1 and ARO cells were incubated in the presence or absence of increasing doses of either ciglitazone (●) or rosiglitazone (■) for 4 d in 10% FCS containing medium, and cell viability was then measured by MTT staining. Only rosiglitazone (■) was used in the remaining three cell lines. Each figure represents the mean ± SD of three separate experiments. B, Cell viability in response to rosiglitazone (ROS, 10 μM) was measured in FF-1, ARO, and HTh74 cells transfected with either siRNA to PPARγ or scrambled siRNA and incubated in the presence or absence of rosiglitazone. PPARγ silencing strongly inhibited rosiglitazone effect on cell viability.

TABLE 1. Effect of either ciglitazone (CIG, 20 μM) or rosiglitazone (ROS, 10 μM) or 9-*cis*-retinoic acid (9cis-RA, 1 μM) on ATC cell viability (MTT staining) when cultured in serum-free medium

Cells	Cell viability (% of untreated)				
	CIG, %	CIG + GW9662	ROS	ROS + GW9662	9cis-RA
FF-1	69 ± 8	98 ± 9	61 ± 4	102 ± 5	85 ± 7
ARO	48 ± 5	99 ± 6	44 ± 3	98 ± 7	72 ± 9
HTh74	59 ± 6	102 ± 5	45 ± 3	97 ± 6	113 ± 6
C643	72 ± 7	104 ± 8	68 ± 7	100 ± 5	111 ± 7
SW1736	65 ± 5	97 ± 7	56 ± 4	98 ± 9	92 ± 11
8305c	61 ± 5	96 ± 9	52 ± 4	99 ± 4	115 ± 16
NPA	95 ± 6	101 ± 8	96 ± 8	98 ± 6	92 ± 13

Preincubation with the PPAR-γ antagonist GW9662 inhibited the effects of PPARγ agonists on cell viability.

simultaneous exposure to 10 μM rosiglitazone markedly increased the effect of doxorubicin in all ATC cells but not in PPARγ-negative NPA cells (Table 2).

PPARγ agonists reduce cell proliferation and cell cycle progression in ATC cells

A cell proliferation reduction, an increased apoptosis rate, or both may explain the reduction of cell viability caused by PPARγ agonists. In a variety of cancer cells, PPARγ inhibits proliferation and cell cycle arrest at G_0/G_1 restriction point. We then evaluated in ATC cells whether rosiglitazone induced these alterations in cell cycle progression. Cells were cultured in the absence or presence of rosiglitazone and synchronized by culturing them for 24 h in leucine-deprived medium, which induces a block at the G_1 restriction point. Cells were then released from the cell cycle block by the addition of regular medium and harvested at 12 h from release. Cell cycle was analyzed by fluorescence-activated cell sorter. Exposure to rosiglitazone differently increased the proportion of cells in G_0/G_1 in the cell lines studied (Table 3). Five cell lines also showed a reduction of the proportion of cells in the S phase. One cell line (C643), however, after exposure to rosiglitazone showed an increased proportion of cells in both G_0/G_1 and S phase with a reduction of the proportion of cells in G_2/M phase (Table 3).

These data strongly suggest that rosiglitazone-induced growth inhibition of ATC cells may be mediated by cell cycle arrest or delay, with cell accumulation in G_0/G_1 phase in most ATC cells.

To evaluate whether overall DNA synthesis was slowed, all six ATC cell lines were exposed to either 10 μM rosiglitazone or 20 μM ciglitazone for 48 h and then subjected to a 4 h ^{3}H-thymidine pulse. ^{3}H-thymidine incorporation was significantly reduced by rosiglitazone in five of six cell lines and by ciglitazone in four of six, confirming that the rate of DNA synthesis is slowed by PPARγ agonists in most ATC cells (Table 4). By contrast, *cis*-retinoic acid reduced ^{3}H-thymidine incorporation in only two cell lines and increased it in one (Table 4).

Because rosiglitazone was able to impair cell cycle progression mainly by blocking cells in G_0/G_1 phase, we evaluated whether rosiglitazone influenced the abundance of critical-negative regulators of cell cycle such as the inhibitors of cyclin-dependent kinases (CDK) inhibitors $p21^{cip1}$ and $p27^{kip1}$, which prevent the phosphorylation of the retinoblastoma protein (Rb) by CDKs and consequently cell cycle progression. Incubation with 10 μM rosiglitazone for 48 h increased the expression level of $p21^{cip1}$ in all ATC cell lines (Fig. 3A). The $p21^{cip1}$ increase ranged from a minimum of approximately 2-fold in FF-1 and 8305c cells to a maximum of approximately 6-fold in C643 cells. Rosiglitazone also induced up-regulation of $p27^{kip1}$ expression in four of six cell lines

TABLE 3. Effect of rosiglitazone (10 μM) on cell cycle distribution in ATC cell lines[a]

Cell line/treatment	Cell cycle phase (%)		
	G_0/G_1	S	G_2/M
FF-1			
Control	52.7 (55.1)	21.4 (23.2)	26.0 (21.7)
Rosiglitazone	57.7 (57.6)	15.3 (19.7)	27.1 (22.7)
ARO			
Control	84.6 (78.3)	9.4 (18.6)	5.9 (4.1)
Rosiglitazone	89.4 (81.1)	5.2 (14.9)	5.4 (4.0)
HTh74			
Control	42.5 (47.6)	30.5 (27.0)	27.0 (25.4)
Rosiglitazone	61.0 (61.7)	6.6 (13.2)	32.4 (25.1)
C643			
Control	64.5 (66.8)	6.0 (13.8)	29.5 (19.4)
Rosiglitazone	71.0 (73.4)	17.2 (18.3)	11.8 (8.2)
SW1736			
Control	49.0 (45.1)	43.0 (49.9)	8.0 (5.0)
Rosiglitazone	67.5 (68.7)	25.1 (26.7)	7.4 (4.6)
8305c			
Control	58.8 (63.7)	11.2 (7.7)	30.0 (28.6)
Rosiglitazone	68.2 (72.9)	4.9 (5.4)	26.9 (21.8)

[a] Data *in parentheses* represent results of a second independent experiment.

TABLE 2. Effect of either rosiglitazone (ROS) or doxorubicin (DOXO) or the combination of the two on cell viability of ATC cells cultured in 10% FCS-containing medium

Cells	Cell viability (percent of untreated)		
	ROS, %[a]	DOXO, %[b]	ROS + DOXO, %
FF-1	88 ± 7	84 ± 8	65 ± 5
ARO	78 ± 5	67 ± 6	37 ± 4
HTh74	77 ± 5	40 ± 3	24 ± 3
C643	81 ± 7	68 ± 9	59 ± 8
SW1736	65 ± 7	94 ± 7	52 ± 4
8305c	62 ± 5	40 ± 5	21 ± 3
NPA	98 ± 5	72 ± 5	71 ± 6

[a] ROS, 10 μM.
[b] DOXO, 0.025 μM in all cells, except HTh74 (0.0125 μM).

TABLE 4. Effect of either ciglitazone (CIG, 20 μM), rosiglitazone (ROS, 10 μM), or 9-*cis*-retinoic acid (9cis-RA, 1 μM) on ^{3}H-thymidine incorporation in ATC cells

Cells	^{3}H-thymidine incorporation (% of untreated)		
	CIG	ROS	9cis-RA
FF-1	59 ± 7	34 ± 5	100 ± 6[a]
ARO	94 ± 8[a]	79 ± 4[a]	89 ± 5[a]
HTh74	83 ± 8[a]	53 ± 7	97 ± 3[a]
C643	76 ± 8	51 ± 6	64 ± 5
SW1736	72 ± 6	46 ± 3	81 ± 7
8305c	71 ± 6	58 ± 5	168 ± 11[b]

[a] Not significantly different from nontreated cells.
Significantly ($P = 0.002$) increased with respect to nontreated cells.

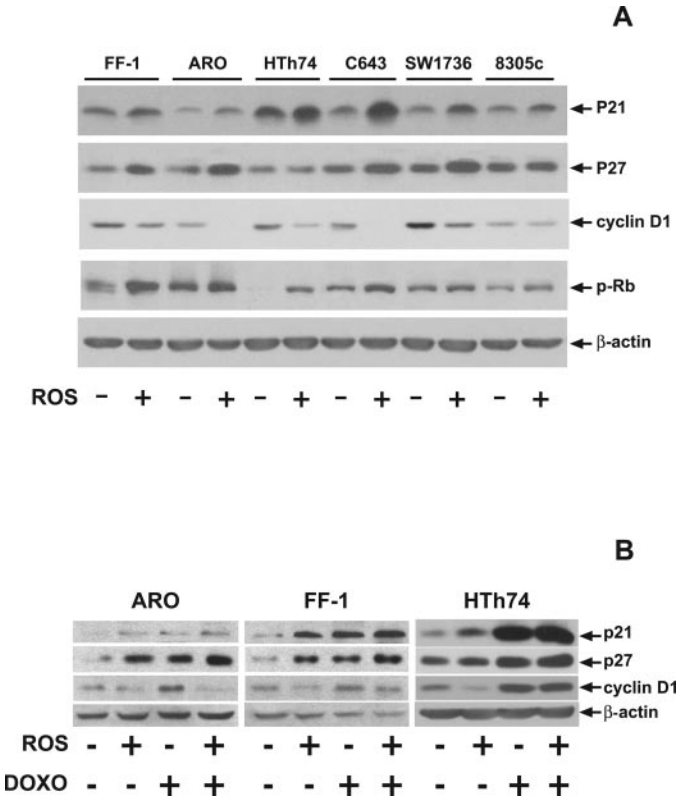

FIG. 3. Effect of rosiglitazone on $p21^{cip1}$, $p27^{kip1}$, and cyclin D1 expression and on Rb phosphorylation. A, ATC cell monolayers were incubated in the presence or absence of 10 μM rosiglitazone (ROS) for 48 h. Cells were then lysed and cell extracts subjected to SDS-PAGE. Protein levels were measured by Western blot analysis with specific antibodies anti-$p21^{cip1}$, anti-$p27^{kip1}$, and anti-cyclin D1 and against the hypophosphorylated (inactive) form of Rb protein, as described in *Materials and Methods*. The experiment shown is representative of three independent experiments. B, Combined effect of 10 μM rosiglitazone (ROS) and doxorubicin (DOXO; 0.0250 μM in ARO and 0.0125 μM in HTh74) on $p21^{cip1}$, $p27^{kip1}$, and cyclin D1 expression.

(Fig. 3A); the increase was maximal in FF-1 and ARO cells (~2.8-fold in both and ~1.8-fold in C643 and SW1736 cells).

We also studied the effect of rosiglitazone on cyclin D1 protein, which plays a critical role in the progression through G_1 to S phase. After 48 h exposure to rosiglitazone, cyclin D1 expression was completely inhibited in ARO and C643 cells. It decreased to less than 20% of untreated in HTh74 cells and approximately 50 and 40% of the untreated in FF-1 and SW1736, respectively. It decreased only slightly in 8305c cells (Fig. 3A).

We then evaluated in ATC cells the phosphorylation status of Rb by using an antibody recognizing the hypophosphorylated (inactive) form of the Rb protein. Exposure to rosiglitazone for 48 h increased the hypophosphorylated form of Rb protein by approximately 2-fold in all cells, except HTh74, in which the hypophosphorylated Rb, expressed at a very low level, was increased by approximately 10-fold after rosiglitazone (Fig. 3A). These data suggest therefore that rosiglitazone inhibits CDK-dependent Rb phosphorylation and subsequent cell cycle progression by increasing $p21^{cip1}$ and/or $p27^{kip1}$ and decreasing cyclin D1 expression levels.

To investigate the mechanisms underlying the potentiation of doxorubicin effect by rosiglitazone, we evaluated the combined effect of doxorubicin and rosiglitazone on cell cycle molecules. Cells were incubated with doxorubicin at the indicated doses in the presence or absence of 10 μM rosiglitazone for 48 h. Doxorubicin was able to increase the expression of $p21^{cip1}$ and $p27^{kip1}$and also rosiglitazone. The greatest increase of both molecules was observed when rosiglitazone and doxorubicin were used in combination (Fig. 3B). Doxorubicin, however, also increased cyclin D1 expression. This increase was partially inhibited by the concomitant exposure to rosiglitazone (Fig. 3B).

PPARγ agonists induce an increased rate of cell apoptosis in ATC cells

We next evaluated whether an increased apoptosis rate may contribute to the reduction of cell viability induced by exposure to PPARγ agonists. Cells were exposed to either rosiglitazone (0.1–10 μM) or ciglitazone (20 μM) for 48 h, and apoptosis was then evaluated by the measure of cytoplasmic histone-associated DNA fragments. PPARγ agonists markedly increased the apoptosis rate in FF-1, HTh74, and C643 cells, whereas they were less effective in SW1736, ARO, and 8305c cells. Rosiglitazone was always more effective than ciglitazone, and its effect was already evident at low doses (0.1–1.0 μM) (Fig. 4). Rosiglitazone effect on ATC cell apoptosis was confirmed by annexin and PI staining in three cell lines (FF-1, ARO, 8305c), in which the effect of rosiglitazone was compared with the effect of staurosporin, a well-known proapoptotic agent (Table 5).

To unravel the molecular mechanisms of the increased apoptosis rate induced by the PPARγ agonists, we studied the effect of rosiglitazone on some apoptosis regulators, such as Bcl-X_L, B-cell leukemia-2 (Bcl-2), Bcl-2-associated X protein (Bax), and second mitochondrion-derived activator (Smac) (also known as Diablo).

The Bcl-2 family includes important apoptosis regulators that can have either proapoptotic (Bax) or antiapoptotic effects (Bcl-2, Bcl-X_L). Exposure to rosiglitazone (10 μM) caused a decrease of Bcl-X_L expression levels in four cell lines, more marked in C643 and 8305c cells (17 and 15% of untreated, respectively) and less marked in FF-1 and HTh74 (60 and 40%, respectively) (Fig. 5A). Rosiglitazone did not affect Bcl-2 and Bax expression levels (Fig. 5A).

Smac is a proapoptotic protein released from the intermembrane space of mitochondria into the cytosol, in which it contributes to activate the mitochondrial apoptosis pathway by inhibiting inhibitor of apoptosis-mediated caspase inhibition. Smac/Diablo was not significantly affected by rosiglitazone (Fig. 5A).

To evaluate the role of caspase activation in rosiglitazone-induced apoptosis, ATC cells were exposed to 10 μM rosiglitazone in the presence or absence of 30 μM of the caspase inhibitor Z-VAD-fmk. Exposure to staurosporin (50 nM), a general tyrosine kinase inhibitor that induces apoptosis and activates caspases (27), was used as positive control. Cell apoptosis was measured by determining cytoplasmic histone-associated DNA fragments, as described in *Materials and Methods*. In all cell lines, both rosiglitazone- and staurosporin-induced apoptosis was almost completely blocked in the presence of Z-VAD-fmk (data not shown).

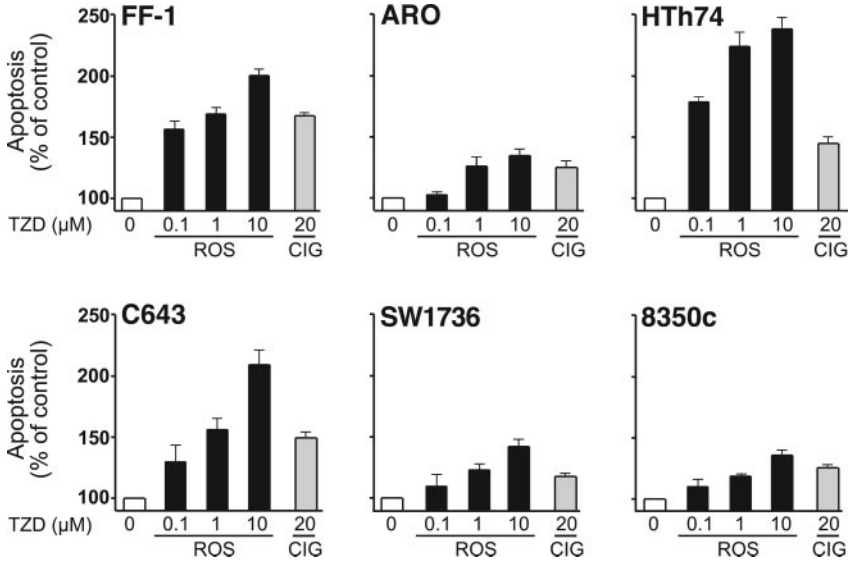

FIG. 4. Effect of ciglitazone and rosiglitazone on ATC cell apoptosis. ATC cells were incubated with either rosiglitazone (ROS) (0.1 to 10 μM) or ciglitazone (CIG) (20 μM) for 48 h. Apoptosis was detected by measuring cytoplasmic histone-associated DNA fragments by ELISA and expressed as percentage of untreated. Data shown represent mean ± SEM of three independent experiments performed in duplicate.

Activation of caspase-3/7 was then measured in rosiglitazone-exposed cells. As shown in Fig. 5B, rosiglitazone significantly ($P < 0.001$) induced caspase-3/7 activation in all cell lines at a level comparable with that induced by 50 nM staurosporin. Caspase-3/7 activation by both rosiglitazone and staurosporin was completely inhibited by 30 μM of Z-VAD-fmk (not shown).

PPARγ agonists inhibit anchorage-independent growth

Anchorage-independent growth is an important feature of the malignant phenotype. We therefore evaluated the effect of PPARγ agonists on anchorage-independent growth by cloning cells in soft agar. Only two cell lines, ARO and SW1736, were able to efficiently form colonies in semisolid agar. At d 5, colonies developed in both the untreated and PPARγ agonist-treated cultures. Colonies were then stained and photographed. Both ciglitazone (20 μM, not shown) and rosiglitazone (10 μM) markedly reduced colony formation in these two cell lines. Figure 6A shows the effect of 10 μM rosiglitazone in ARO cells. Dose-response experiments showed that this inhibiting effect was already evident at doses as low as 0.1 μM PPARγ agonists (not shown).

TABLE 5. Annexin and PI staining in ATC cell lines exposed to either rosiglitazone (4 d) or staurosporin (2 h)

Cell line/treatment	Cells (%)		
	Living	Annexin^{+ve}	Propidium^{+ve}
FF-1			
Control	61.5 ± 5	36.8 ± 4	1.7 ± 2
Rosiglitazone	23.9 ± 4[a]	61.1 ± 5[b]	1.5 ± 3
Staurosporin	47.4 ± 7[b]	48.9 ± 4[b]	3.7 ± 4
ARO			
Control	52.2 ± 4	41.9 ± 4	5.9 ± 3
Rosiglitazone	29.6 ± 3[a]	60.8 ± 3[c]	9.6 ± 1
Staurosporin	13.3 ± 5[a]	61.6 ± 8[c]	25.1 ± 9
8305c			
Control	66.0 ± 6	33.3 ± 5	0.7 ± 5
Rosiglitazone	46.4 ± 6[c]	50.4 ± 7[c]	3.2 ± 2
Staurosporin	17.5 ± 4[a]	77.6 ± 9[a]	4.9 ± 3

Data represent mean ± SD of three independent experiments, each carried out in duplicate.
[a] $P < 0.0001$.
[b] $P < 0.02$.
[c] $P < 0.008$ (statistically different from control by Student's t test).

PPARγ agonists antagonize biological effects of IGF-I in ATC cells by inhibiting Akt phosphorylation and up-regulating PTEN

In thyroid cancer cells, the IGF system is overactivated by multiple mechanisms, and the biological effects of IGFs appear to be important in thyroid cancer progression by stimulating growth, resistance to apoptosis, and cell migration (7, 8). We therefore evaluated whether PPARγ agonists affected IGF-I effects in ATC cells. When cell monolayers were stimulated with 10 nM IGF-I, cell density increased from 131 to 211%, as evaluated by MTT assay; 10 μM rosiglitazone completely blocked this effect (data not shown).

When ARO cells were seeded in semisolid agar in the presence of a reduced amount of serum (2% charcoal-stripped serum), IGF-I was able to stimulate both the number and size of colonies. This IGF-I effect was also completely blocked by the presence of rosiglitazone (10 μM) (Fig. 6B). Most biological effects of IGF-I are responsive to the activation of the insulin receptor substrate (IRS)-1/PI3K/Akt pathway. We therefore evaluated whether LY294002, an inhibitor of PI3K, affected IGF-I-stimulated colony formation. In fact, IGF-I effect was abolished by LY294002 (5 μM) (Fig. 6B). In these culture conditions, the effect of both LY294002 and rosiglitazone was minimal in the absence of IGF-I (not shown).

We also evaluated the effect of rosiglitazone on cell migration in Boyden chambers in response to IGF-I used as chemoattractant. Both the basal and IGF-I stimulated cell migration were significantly inhibited by rosiglitazone in all ATC cell lines (Fig. 7). Incubation with LY294002 (5 μM) also blocked the effect of IGF-I on cell migration (Fig. 7). Taken together these data indicate that IGF-I-induced biological effects such as colony formation and cell migration are PI3K dependent and are inhibited by rosiglitazone.

We therefore evaluated whether rosiglitazone affected the

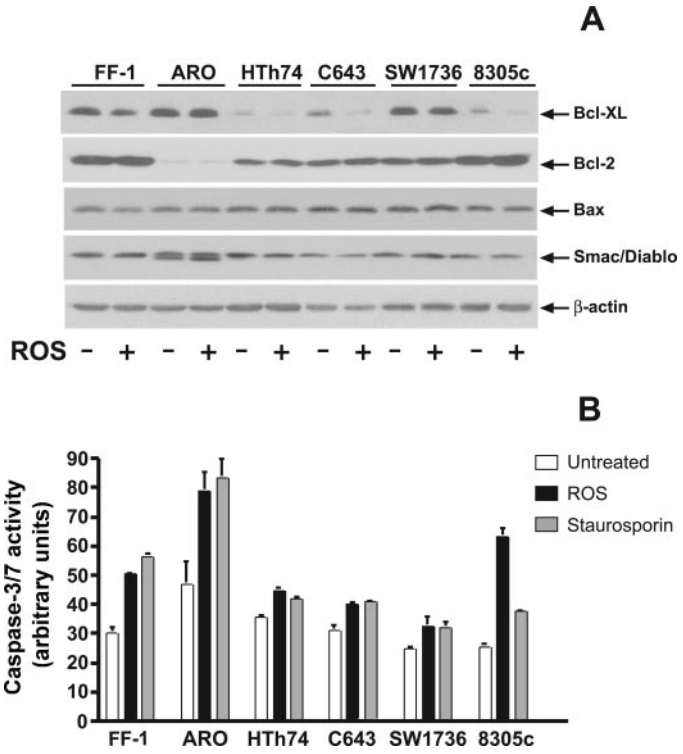

FIG. 5. A, Effect of rosiglitazone on Bcl-2, Bcl-X_L, Bax, and Smac/Diablo content. Cell monolayers were incubated in the presence or absence of 10 μM rosiglitazone (ROS) for 48 h. Cells were then lysed and cell extracts subjected to SDS-PAGE. Protein levels were measured by Western blot analysis with specific antibodies anti-Bcl-2, anti-Bcl-X_L, anti-Bax, and anti-Smac/Diablo, as described in *Materials and Methods*. The experiment shown is representative of three independent experiments. B, Activation of caspase-3/7 in response to rosiglitazone. Cell monolayers were incubated in the presence or absence of either 10 μM rosiglitazone (ROS) for 48 h or 50 nM staurosporin. Activation of caspase-3/7 was then evaluated, as described in *Materials and Methods*. The experiment shown is representative of three independent experiments and represents mean ± SEM of duplicates.

activation of the IRS/PI3K/Akt pathway in response to IGF-I. Cell incubation with 10 μM rosiglitazone did not have any major effect on IGF-I receptors (IGF-IRs), which were slightly reduced in ARO and HTh74 cells and unaffected in the remaining cell lines (Fig. 8A). IRS-1 was clearly up-regulated in three cell lines (FF-1, HTh74, and SW1736), whereas IRS-2 content was unaffected (Fig. 8A).

Akt activation was then measured by Western blot analysis using phospho-specific antibodies to phosphorylated Ser473 and Thr308 of Akt in ATC cells preincubated or not with 10 μM rosiglitazone for 48 h and then stimulated with 10 nM IGF-I for 10 min. IGF-I-induced Akt Ser473 phosphorylation was slightly but consistently decreased by rosiglitazone in FF-1 and ARO cells (~80% of untreated in both) and markedly decreased in HTh74, C643, and 8305c cells (~50% of untreated in all three of them) (Fig. 8B). Very similar results were obtained with an antibody to phosphorylated Thr308 of Akt (not shown). In contrast to Akt, IRS-1 phosphorylation reflected IRS-1 expression levels and was increased by rosiglitazone in FF-1, HTh74, and SW1736, indicating that IRS-1 was functional and not responsible for the inhibition of Akt phosphorylation by rosiglitazone (Fig. 8B).

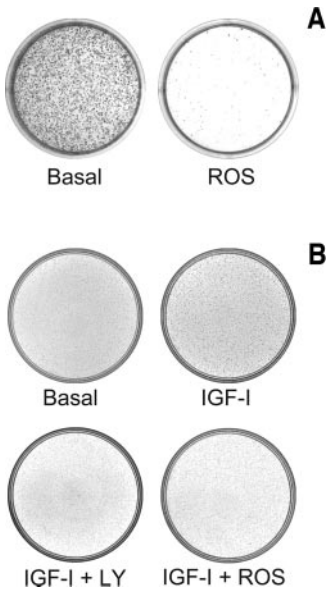

FIG. 6. Effect of rosiglitazone on anchorage-independent cell growth in ARO cells. A, ARO cells were seeded in soft agar containing 10% FCS in the presence or absence of 10 μM rosiglitazone (ROS). At d 5, colonies were then stained by *p*-iodonitrotetrazolium violet and photographed. B, ARO cells were seeded in soft agar in 2% charcoal-stripped FCS containing medium and incubated in the presence or absence of 10 nM IGF-I with or without 10 μM rosiglitazone (ROS) or 5 μM LY294002 (LY). At d 5, colonies were then stained and photographed.

The ratio phospho-IRS-1/phospho-Akt was therefore increased in rosiglitazone-treated cells, compared with untreated cells (Fig. 8B).

Time-course experiments revealed that Akt phosphorylation (both Ser473 and Thr308) was reduced, especially as far as peak values are concerned. In untreated FF-1 cells, Akt phosphorylation at Ser473 remained clearly detectable at 180 min, whereas it was almost switched off after 80 min in rosiglitazone-treated cells (Fig. 8C). Similar results were obtained in HTh74 and C643 cells (data not shown).

The Akt pathway is negatively regulated by the lipid phosphatase PTEN, which is an important antioncogene. In cells exposed to rosiglitazone, PTEN was clearly up-regulated in all cell lines, ranging from 148 ± 12 to 414 ± 27% of untreated cells (Fig. 9). These data indicate that PTEN up-regulation and subsequent inhibition of Akt phosphorylation could be involved in the inhibition by rosiglitazone of the ATC cell biological responses to IGF-I.

Increase of thyroid-specific differentiation markers by PPARγ agonists

Because PPARγ agonists have been reported to promote differentiation in certain cancer cells, we evaluated whether rosiglitazone increased the expression of thyroid-specific differentiation markers, such as Tg, TSH-R, NIS and TPO, in ATC cells. After incubation with 10 μM rosiglitazone for 48 h, mRNA for Tg, TSH-R, NIS, and TPO was measured by quantitative real-time PCR. As shown in Fig. 10, exposure to rosiglitazone increased the expression of these thyroid-specific molecules in ATC cell lines. No significant effect was

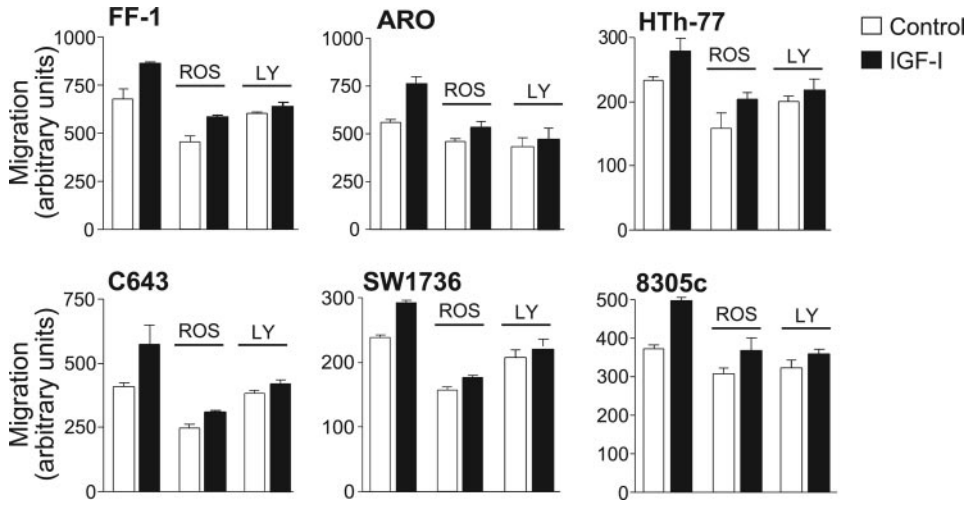

FIG. 7. Effect of rosiglitazone on IGF-I-stimulated cell migration. ATC cells were seeded at the top of Boyden chambers coated at the lower side with 250 μg/ml collagen IV in the presence or absence of 10 μM rosiglitazone (ROS) or 5 μM LY294002 (LY) and cell migration stimulated with 10 nM IGF-I (■) or serum-free medium (□) in the lower chamber for 18 h. The migrated cells were stained as described in *Materials and Methods*. *Bars* represent the mean ± SD of triplicate experiments.

observed in NPA papillary cancer cells, whereas PPARγ was undetectable and nonfunctional.

Discussion

The main findings of our study indicate that ATC cells express functional PPARγ protein and that, in these cells, PPARγ agonists induce pleiotropic effects consistent with a partial reversion of the EMT, highly characteristic of this aggressive carcinoma.

Biological effects elicited by PPARγ agonists in ATC cells included: 1) inhibition of anchorage-dependent and -independent growth and inhibition of cell cycle progression at G_0/G_1 phase; 2) potentiation of doxorubicin effects; 3) inhibition of cell migration; 4) increased apoptosis rate; 5) down-regulation of the IGF system; and 6) increase of expression of thyroid-specific differentiation markers. These effects will be discussed separately.

PPARγ agonists reduced ATC cell viability by inducing both growth arrest and an increased apoptosis rate. They also dramatically reduced anchorage-independent growth by reducing both colony number and size. In addition, our study indicates that PPARγ agonists inhibit cell cycle progression in ATC cells by multiple mechanisms, resulting in ATC cell accumulation in G_0/G_1 phase. The progression in the cell cycle requires cyclin/CDK complexes that result in phosphorylation of the Rb protein. Upon phosphorylation, Rb releases the transcription factor E2F that activates transcription of genes involved in cell cycle progression (26, 27). Rosiglitazone increased the hypophosphorylated (inactive) form of Rb protein, a likely consequence of the effects of up-regulation of CDK inhibitors and down-regulation of cyclin D1. Cyclin/CDK complexes are negatively regulated by CDK inhibitors, in particular $p21^{Cip1}$ and $p27^{Kip1}$, that have a key role in mediating G_1 arrest by inhibiting cyclin D1-CDK4 and other cyclin/CDK complexes (26–29). Rosiglitazone up-regulated both $p21^{Cip1/Waf1}$ and $p27^{Kip1}$. $p21^{Cip1/Waf1}$ is normally induced by p53 and is a key mediator of p53-mediated G_1 arrest (30). However, $p21^{Cip1/Waf1}$ may also be induced by p53-independent mechanisms. The ATC cell lines examined in the present study express either a mutated p53 (31) or do not express p53 (SW1736 cells); therefore, the rosiglitazone-mediated $p21^{Cip1/Waf1}$ up-regulation found in ATC cells appears to be p53 independent. This observation is relevant in view to the fact that p53 is frequently mutated in human ATCs and that p53 mutations are believed to play a role in thyroid cancer dedifferentiation (34).

TZDs had already been reported to influence CDK inhibitors: troglitazone may induce up-regulation of both $p21^{Cip1/Waf1}$ and $p27^{Kip1}$ in thyroid cancer cells and pancreatic cells (14, 33), whereas ciglitazone may up-regulate $p27^{Kip1}$, but not $p21^{Cip1/Waf1}$, in thyroid cancer cells (34) and $p27^{Kip1}$ and $p18^{INK4c}$ in hepatocellular carcinoma (35, 36). However, this p53-independent effect of TZDs on CDK inhibitors is a novel observation to our knowledge.

We also demonstrate that rosiglitazone down-regulated cyclin D1 protein in ATC cells. Cyclin D1 is a rate-limiting factor in cell proliferation induced by growth factors in various models and is often overexpressed in cancer cells in which it is induced by several oncogenes and functions as a collaborative oncogene (37–39). Previous studies carried out in other cell models have reported that PPARγ agonists may down-regulate cyclin D1 expression by both inducing proteasome-dependent degradation of the protein (40) and inhibiting its transcription (41).

In addition to cell growth inhibition, PPARγ agonists increased ATC cells apoptosis rate. These findings are in agreement with the results of other authors, who showed a predominant apoptotic effect of PPARγ agonists in different anaplastic thyroid cancer cells (42). We found that rosiglitazone-induced apoptosis was associated in most ATC cells with the down-regulation of $Bclx_L$ an antiapoptotic protein of the Bcl-2 family. Bcl2 and Bax were unaffected. Rosiglitazone also caused caspase-3/7 activation, and incubation with the caspase inhibitor Z-VAD-fmk reduced rosiglitazone-induced apoptosis. Also, these are novel findings, although it has been previously reported that Bcl2 may be down-regulated by PPARγ agonists in breast and colon cancer and glioblastoma (43–45).

Interestingly, rosiglitazone potentiated the effect of low doses of doxorubicin, a chemotherapeutic drug frequently used in the therapy of ATC, on cell growth and survival.

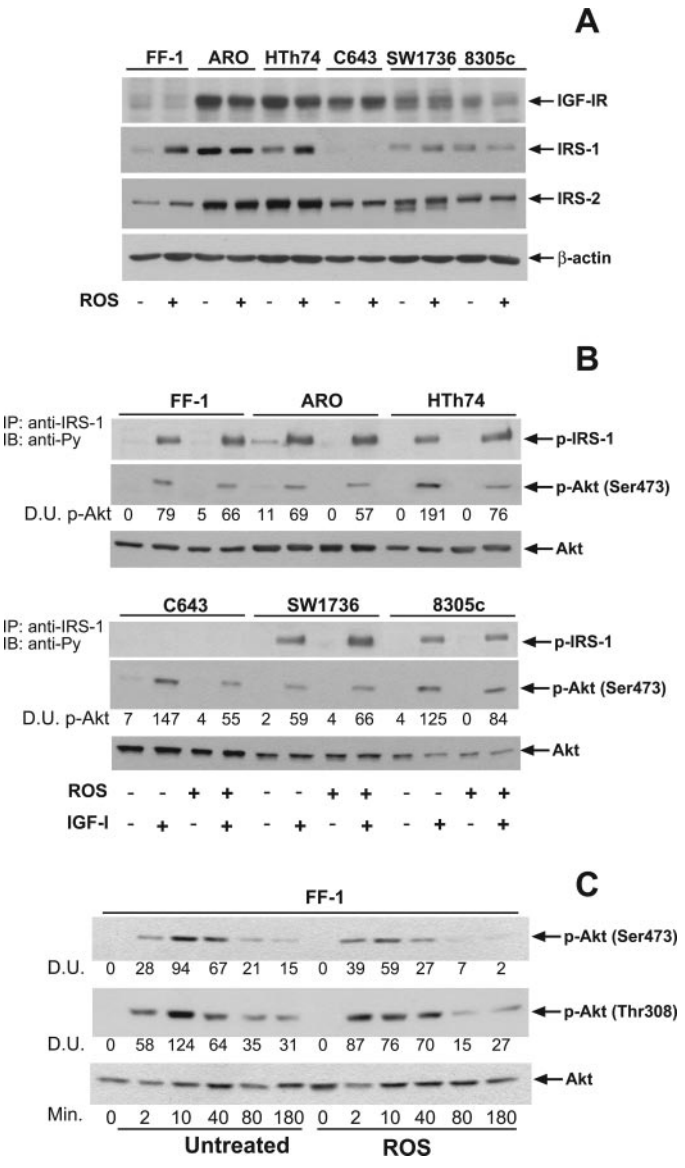

FIG. 8. A, Effect of rosiglitazone on IGFI-R, IRS-1, and IRS-2 expression. Cell monolayers were incubated in the presence or absence of 10 μM rosiglitazone (ROS) for 48 h. Cells were then lysed and cell extracts subjected to SDS-PAGE. Protein levels were measured by Western blot analysis with specific antibodies anti-IRS-1 or anti-IRS-2, as described in *Materials and Methods*. The experiment shown is representative of three independent experiments. B, Effect of rosiglitazone on IRS-1 and Akt phosphorylation in response to IGF-1. Serum-starved cell monolayers, preincubated in the presence or absence of 10 μM rosiglitazone (ROS) for 48 h, were stimulated with 10 nM IGF-I for 10 min. For IRS-1 phosphorylation, cell lysates were immunoprecipitated (IP) with an anti-IRS-1 antibody and subjected to SDS-PAGE. Blots were then incubated with an anti-Py antibody. For Akt phosphorylation, whole-cell lysates were subjected to SDS-PAGE. Blots were incubated with a phospho-specific antiphospho Akt (Ser473) and then stripped and sequentially incubated with an anti-Akt antibody, as described in *Materials and Methods*. The experiment shown is representative of three independent experiments. Values representing densitometric reading of phospho-Akt signal are indicated as D.U. (densitometric units). IB, Immunoblot. C, Time-course Akt activation at Ser473 and Thr308 phosphorylation sites after IGF-I in rosiglitazone-treated and untreated FF-1 cells. Values representing densitometric reading of phospho-Akt signal are indicated as D.U.

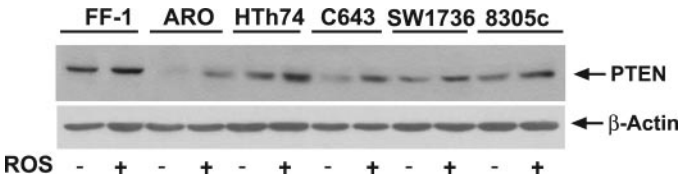

FIG. 9. Effect of rosiglitazone on PTEN expression. Cell monolayers were incubated in the presence or absence of 10 μM rosiglitazone (ROS) for 48 h and PTEN expression measured by Western blot with an anti-PTEN antibody. The experiment shown is representative of three independent experiments.

Interestingly, both rosiglitazone and doxorubicin up-regulated $p21^{Cip1/Waf1}$ and $p27^{Kip1}$, and the combination of the two compounds had an additive effect. These data suggest that this drug combination may improve the outcome of ATC patients. These data are in agreement with a very recent report showing that a novel PPARγ agonist (RS5444) alone and in combination with paclitaxel inhibits *in vitro* and *in vivo* growth of two different ATC cell lines by up-regulating $p21^{Cip1/Waf1}$ (46).

The ability of cancer cells to migrate and invade the endothelial basal membrane is a prerequisite to develop local invasion and metastatic spreading. ATC is characterized by massive invasion of nearby structures and early development of locoregional and distant metastases. The markedly reduced ATC cell migration caused by rosiglitazone is an intriguing finding and is reminiscent of chemotaxis inhibition of vascular smooth muscle cells and monocytes by

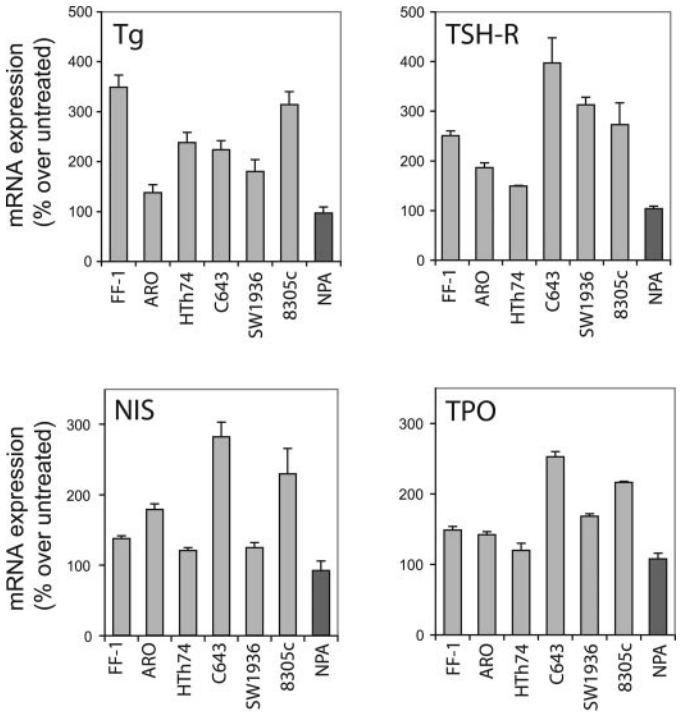

FIG. 10. Effect of rosiglitazone on the expression of thyroid-specific differentiation markers. ATC and NPA cells were incubated in the presence or absence of rosiglitazone (10 μM) for 48 h. mRNA for Tg, TSH-R, NIS, and TPO was then measured by quantitative real-time PCR, as described in *Materials and Methods*. Results are given as percentage of untreated cells. The experiment shown represents mean ± SD of three independent experiments.

PPARγ agonists (47, 48). One possible mechanism is Ets-1 transrepression (49), which is known to regulate matrix metalloproteinase-9 and other matrix metalloproteinases that allow digestion of extracellular matrix (50).

An additional antineoplastic mechanism of TZDs in ATC cells is the antagonist effect on IGF-I. Many features of malignant cells, such as unregulated growth and apoptosis and enhanced cell invasion, are modulated by growth factors and cytokines produced in an autocrine or paracrine manner. Among growth factors produced by ATC, IGF-I, and IGF-II have a crucial role in thyroid cancer progression through the activation of their cognate receptor IGF-IR and insulin receptor isoform A (6), which have a mitogenic, antiapoptotic, and transforming potential (51). Rosiglitazone antagonized major biological effects of IGF-I, such as cell migration, survival, and anchorage-independent growth. A possible mechanism for this antagonist effect is the inhibition of the PI3K/Akt pathway by PTEN up-regulation. The PI3K/Akt pathway is a major pathway activated by IGF-I and plays a key role in mediating its biological effects (52). This pathway is negatively regulated by the lipid phosphatase PTEN that dephosphorylates the PI3K product phosphatidylinositol-(3,4,5,)-triphosphate, which, in turn, activates Akt and other downstream kinases (53). The concomitant Akt inhibition and PTEN up-regulation in response to PPARγ agonists have already been reported in pancreatic cancer cells (54).

Finally, rosiglitazone increased the expression of thyroid-specific differentiation markers, such as Tg, TSH-R, NIS and TPO, indicating a partial redifferentiation effect. Our results are in agreement with those of others showing that troglitazone increases iodine uptake by cultured follicular cancer cell lines *in vitro* (55, 56) and that rosiglitazone administration in patients with metastatic thyroid cancer may increase Tg production and radioiodine uptake, albeit at a low degree, by the metastatic tissue (57).

These multiple molecular effects of TZDs affected ATC cell phenotype, inducing morphological (more polygonal, epithelial-like cell morphology; data not shown) changes that are typical of thyroid cell epithelial differentiation and EMT reversal.

It has been reported that some antitumor effects of TZDs are PPARγ independent, at least in certain cell models (58, 59). In our system, however, different lines of evidence indicate that the biological effects of TZDs described here require a functional PPARγ. First, these effects occurred at doses of rosiglitazone as low as 0.1 μM and only in cells expressing a functional PPARγ, whereas they were not observed in PPARγ-negative NPA papillary cancer cells. Second, they were inhibited by specific siRNA to PPARγ and pretreatment with GW9662, a potent and selective antagonist of PPARγ that causes specific and irreversible loss of binding. However, there was no strict correlation between PPARγ expression and functional level and the molecular and biological response to TZDs in the different ATC cells lines. This is not surprising because the selective transactivation of the different genes by PPARγ activation may vary in the different cells and tissues according to the nature of PPRE in the upstream regions of target genes and the relative abundance of coactivators and corepressors and other nuclear transcription factors that may either compete or cross-talk with PPARγ and its heterodimerization partner retinoid X receptor (60). Moreover, the relationship between gene regulation by PPARγ and biological effects is obviously affected by the numerous abnormalities in growth and apoptosis regulatory genes present in the different ATC cell lines. However, in all cell lines studied, PPARγ agonists had similar antiproliferative, proapoptotic, and differentiating effects.

In conclusion, our data indicate that PPARγ agonists induce a partial reversion of the epithelial mesenchymal transition in ATC cells by multiple mechanisms. These effects occur independently of a functional p53, often mutated in ATC, and include partial antagonism with IGF-I effects. Furthermore, because PPARγ agonists potentiate the effect of doxorubicin, the most frequently used chemotherapeutic drug in patients with ATC, they may have a clinical role in the multimodal therapy currently used to slow down ATC growth and dissemination.

Acknowledgments

Received December 19, 2005. Accepted June 6, 2006.

Address all correspondence and requests for reprints to: Antonino Belfiore, M.D., Dipartimento di Medicina Sperimentale e Clinica, Cattedra di Endocrinologia, Università di Catanzaro, v.le Europa, Loc. Germaneto, 88100 Catanzaro, Italy. E-mail: belfiore@unicz.it.

This work was supported by grants from the Associazione Italiana per la Ricerca sul Cancro (to A.B. and R.V.) and Ministero Italiano Università e Ricerca (Cofin 2003 and 2005) (to A.B.).

References

1. **Ain KB** 2000 Management of undifferentiated thyroid cancer. Baillieres Best Pract Res Clin Endocrinol Metab 14:615–629
2. **Veness MJ, Porter GS, Morgan GJ** 2004 Anaplastic thyroid carcinoma: dismal outcome despite current treatment approach. ANZ J Surg 74:559–562
3. **Morali OG, Delmas V, Moore R, Jeanney C, Thiery JP, Larue L** 2001 IGF-II induces rapid β-catenin relocation to the nucleus during epithelium to mesenchyme transition. Oncogene 20:4942–4950
4. **Thiery JP** 2002 Epithelial-mesenchymal transitions in tumour progression. Nat Rev Cancer 2:442–454.
5. **Vella V, Sciacca L, Pandini G, Mineo R, Squatrito S, Vigneri R, Belfiore A** 2001 The IGF system in thyroid cancer: new concepts. Mol Pathol 54:121–124
6. **Vella V, Pandini G, Sciacca L, Mineo R, Vigneri R, Pezzino V, Belfiore A** 2002 A novel autocrine loop involving IGF-II and the insulin receptor isoform-A stimulates growth of thyroid cancer. J Clin Endocrinol Metab 87:245–254
7. **Rosen ED, Spiegelman BM** 2001 PPARγ : a nuclear regulator of metabolism, differentiation, and cell growth. J Biol Chem 276:37731–37734
8. **Yki-Jarvinen H** 2004 Thiazolidinediones N Engl J Med 351:1106–1118
9. **Burstein HJ, Demetri GD, Mueller E, Sarraf P, Spiegelman BM, Winer EP** 2003 Use of the peroxisome proliferator-activated receptor (PPAR) γ ligand troglitazone as treatment for refractory breast cancer: a phase II study. Breast Cancer Res Treat 79:391–397
10. **Butler R, Mitchell SH, Tindall DJ, Young CY** 2000 Nonapoptotic cell death associated with S-phase arrest of prostate cancer cells via the peroxisome proliferator-activated receptor γ ligand, 15-deoxy-Δ12,14-prostaglandin J2. Cell Growth Differ 11:49–61
11. **Chang TH, Szabo E** 2000 Induction of differentiation and apoptosis by ligands of peroxisome proliferator-activated receptor γ in non-small cell lung cancer. Cancer Res 60:1129–1138
12. **Heaney AP, Fernando M, Yong WH, Melmed S** 2002 Functional PPARγ receptor is a novel therapeutic target for ACTH-secreting pituitary adenomas. Nat Med 8:1281–1287
13. **Inoue K, Kawahito Y, Tsubouchi Y, Kohno M, Yoshimura R, Yoshikawa T, Sano H** 2001 Expression of peroxisome proliferator-activated receptor γ in renal cell carcinoma and growth inhibition by its agonists. Biochem Biophys Res Commun 287:727–732
14. **Kawa S, Nikaido T, Unno H, Usuda N, Nakayama K, Kiyosawa K** 2002 Growth inhibition and differentiation of pancreatic cancer cell lines by PPARγ ligand troglitazone. Pancreas 24:1–7
15. **Li MY, Deng H, Zhao JM, Dai D, Tan XY** 2003 Peroxisome proliferator-activated receptor γ ligands inhibit cell growth and induce apoptosis in human liver cancer BEL-7402 cells. World J Gastroenterol 9:1683–1688
16. **Mueller E, Smith M, Sarraf P, Kroll T, Aiyer A, Kaufman DS, Oh W, Demetri**

G, Figg WD, Zhou XP, Eng C, Spiegelman BM, Kantoff PW 2000 Effects of ligand activation of peroxisome proliferator-activated receptor γ in human prostate cancer. Proc Natl Acad Sci USA 97:10990–10995
17. **Shimada T, Kojima K, Yoshiura K, Hiraishi H, Terano A** 2002 Characteristics of the peroxisome proliferator activated receptor γ (PPARγ) ligand induced apoptosis in colon cancer cells. Gut 50:658–664
18. **Kroll TG, Sarraf P, Pecciarini L, Chen CJ, Mueller E, Spiegelman BM, Fletcher JA** 2000 PAX8-PPARγ1 fusion oncogene in human thyroid carcinoma. Science 289:1357–1360
19. **Kato Y, Ying H, Zhao L, Furuya F, Araki O, Willingham MC, Cheng SY** 2006 PPARγ insufficiency promotes follicular thyroid carcinogenesis via activation of the nuclear factor-κB signaling pathway. Oncogene 25:2736–2747
20. **Kurebayashi J, Tanaka K, Otsuki T, Moriya T, Kunisue H, Uno M, Sonoo H** 2000 All-trans-retinoic acid modulates expression levels of thyroglobulin and cytokines in a new human poorly differentiated papillary thyroid carcinoma cell line, KTC-1. J Clin Endocrinol Metab 85:2889–2896
21. **Grunwald F, Menzel C, Bender H, Palmedo H, Otte R, Fimmers R, Risse J, Biersack HJ** 1998 Redifferentiation therapy-induced radioiodine uptake in thyroid cancer. J Nucl Med 39:1903–1906
22. **Heo DS, Park JG, Hata K, Day R, Herberman RB, Whiteside TL** 1990 Evaluation of tetrazolium-based semiautomatic colorimetric assay for measurement of human antitumor cytotoxicity. Cancer Res 50:3681–3690
23. **Kliewer SA, Forman BM, Blumberg B, Ong ES, Borgmeyer U, Mangelsdorf DJ, Umesono K, Evans RM** 1994 Differential expression and activation of a family of murine peroxisome proliferator-activated receptors. Proc Natl Acad Sci USA 91:7355–7359
24. **Ginzinger DG** 2002 Gene quantification using real-time quantitative PCR: an emerging technology hits the mainstream. Exp Hematol 30:503–512
25. **Tikhomirov O, Carpenter G** 2001 Caspase-dependent cleavage of ErbB-2 by geldanamycin and staurosporin. J Biol Chem 276:33675–33680
26. **Nevins JR** 2001 The Rb/E2F pathway and cancer. Hum Mol Genet 10:699–703
27. **Frolov MV, Dyson NJ** 2004 Molecular mechanisms of E2F-dependent activation and pRB-mediated repression. J Cell Sci 117:2173–2181
28. **el-Deiry WS, Tokino T, Velculescu VE, Levy DB, Parsons R, Trent JM, Lin D, Mercer WE, Kinzler KW, Vogelstein B** 1993 WAF1, a potential mediator of p53 tumor suppression. Cell 75:817–825
29. **Polyak K, Lee MH, Erdjument-Bromage H, Koff A, Roberts JM, Tempst P, Massague J** 1994 Cloning of p27Kip1, a cyclin-dependent kinase inhibitor and a potential mediator of extracellular antimitogenic signals. Cell 78:59–66
30. **Waldman T, Kinzler KW, Vogelstein B** 1995 p21 is necessary for the p53-mediated G_1 arrest in human cancer cells. Cancer Res 55:5187–5190
31. **Frasca F, Vella V, Aloisi A, Mandarino A, Mazzon E, Vigneri R, Vigneri P** 2003 p73 tumor-suppressor activity is impaired in human thyroid cancer. Cancer Res 63:5829–5837
32. **Fagin JA, Matsuo K, Karmakar A, Chen DL, Tang SH, Koeffler HP** 1993 High prevalence of mutations of the p53 gene in poorly differentiated human thyroid carcinomas. J Clin Invest 91:179–184
33. **Chung SH, Onoda N, Ishikawa T, Ogisawa K, Takenaka C, Yano Y, Hato F, Hirakawa K** 2002 Peroxisome proliferator-activated receptor γ activation induces cell cycle arrest via the p53-independent pathway in human anaplastic thyroid cancer cells. Jpn J Cancer Res 93:1358–1365
34. **Martelli ML, Iuliano R, Le Pera I, Sama I, Monaco C, Cammarota S, Kroll T, Chiariotti L, Santoro M, Fusco A** 2002 Inhibitory effects of peroxisome proliferator-activated receptor γ on thyroid carcinoma cell growth. J Clin Endocrinol Metab 87:4728–4735
35. **Rumi MA, Sato H, Ishihara S, Ortega C, Kadowaki Y, Kinoshita Y** 2002 Growth inhibition of esophageal squamous carcinoma cells by peroxisome proliferator-activated receptor-γ ligands. J Lab Clin Med 140:17–26
36. **Satoh T, Toyoda M, Hoshino H, Monden T, Yamada M, Shimizu H, Miyamoto K, Mori M** 2002 Activation of peroxisome proliferator-activated receptor-γ stimulates the growth arrest and DNA-damage inducible 153 gene in non-small cell lung carcinoma cells. Oncogene 21:2171–2180
37. **Kenny FS, Hui R, Musgrove EA, Gee JM, Blamey RW, Nicholson RI, Sutherland RL, Robertson JF** 1999 Overexpression of cyclin D1 messenger RNA predicts for poor prognosis in estrogen receptor-positive breast cancer. Clin Cancer Res 5:2069–2076
38. **Pestell RG, Albanese C, Reutens AT, Segall JE, Lee RJ, Arnold A** 1999 The cyclins and cyclin-dependent kinase inhibitors in hormonal regulation of proliferation and differentiation. Endocr Rev 20:501–534
39. **Lee RJ, Albanese C, Fu M, D'Amico M, Lin B, Watanabe G, Haines 3rd GK, Siegel PM, Hung MC, Yarden Y, Horowitz JM, Muller WJ, Pestell RG** 2000 Cyclin D1 is required for transformation by activated Neu and is induced through an E2F-dependent signaling pathway. Mol Cell Biol 20:672–683
40. **Qin C, Burghardt R, Smith R, Wormke M, Stewart J, Safe S** 2003 Peroxisome proliferator-activated receptor γ agonists induce proteasome-dependent degradation of cyclin D1 and estrogen receptor α in MCF-7 breast cancer cells. Cancer Res 63:958–964
41. **Wang C, Fu M, D'Amico M, Albanese C, Zhou JN, Brownlee M, Lisanti MP, Chatterjee VK, Lazar MA, Pestell RG** 2001 Inhibition of cellular proliferation through IκB kinase-independent and peroxisome proliferator-activated receptor γ-dependent repression of cyclin D1. Mol Cell Biol 21:3057–3070
42. **Hayashi N, Nakamori S, Hiraoka N, Tsujie M, Xundi X, Takano T, Amino N, Sakon M, Monden M** 2004 Antitumor effects of peroxisome proliferator activate receptor γ ligands on anaplastic thyroid carcinoma. Int J Oncol 24: 89–95
43. **Elstner E, Muller C, Koshizuka K, Williamson EA, Park D, Asou H, Shintaku P, Said JW, Heber D, Koeffler HP** 1998 Ligands for peroxisome proliferator-activated receptor-γ and retinoic acid receptor inhibit growth and induce apoptosis of human breast cancer cells *in vitro* and in BNX mice. Proc Natl Acad Sci USA 95:8806–8811
44. **Chen GG, Lee JF, Wang SH, Chan UP, Ip PC, Lau WY** 2002 Apoptosis induced by activation of peroxisome-proliferator activated receptor-γ is associated with Bcl-2 and NF-κB in human colon cancer. Life Sci 70:2631–2646
45. **Kim EJ, Park KS, Chung SY, Sheen YY, Moon DC, Song YS, Kim KS, Song S, Yun YP, Lee MK, Oh KW, Yoon do Y, Hong JT** 2003 Peroxisome proliferator-activated receptor-γ activator 15-deoxy-Δ12,14-prostaglandin J2 inhibits neuroblastoma cell growth through induction of apoptosis: association with extracellular signal-regulated kinase signal pathway. J Pharmacol Exp Ther 307:505–517
46. **Copland JA, Marlow LA, Kurakata S, Fujiwara K, Wong AK, Kreinest PA, Williams SF, Haugen BR, Klopper JP, Smallridge RC** 2006 Novel high-affinity PPARγ agonist alone and in combination with paclitaxel inhibits human anaplastic thyroid carcinoma tumor growth via p21(WAF1/CIP1). Oncogene 25:2304–2317
47. **Hsueh WA, Jackson S, Law RE** 2001 Control of vascular cell proliferation and migration by PPARγ: a new approach to the macrovascular complications of diabetes. Diabetes Care 24:392–397
48. **Hornung D, Waite LL, Ricke EA, Bentzien F, Wallwiener D, Taylor RN** 2001 Nuclear peroxisome proliferator-activated receptors α and γ have opposing effects on monocyte chemotaxis in endometriosis. J Clin Endocrinol Metab 86:3108–3114
49. **Ricote M, Li AC, Willson TM, Kelly CJ, Glass CK** 1998 The peroxisome proliferator-activated receptor-γ is a negative regulator of macrophage activation. Nature 391:79–82
50. **Goetze S, Xi XP, Kawano H, Gotlibowski T, Fleck E, Hsueh WA, Law RE** 1999 PPAR γ-ligands inhibit migration mediated by multiple chemoattractants in vascular smooth muscle cells. J Cardiovasc Pharmacol 33:798–806
51. **Valentinis B, Baserga R** 2001 IGF-I receptor signalling in transformation and differentiation. Mol Pathol 54:133–137
52. **Navarro M, Baserga R** 2001 Limited redundancy of survival signals from the type 1 insulin-like growth factor receptor. Endocrinology 142:1073–1081
53. **Maehama T, Dixon JE** 1999 PTEN: a tumour suppressor that functions as a phospholipid phosphatase. Trends Cell Biol 9:125–128
54. **Patel L, Pass I, Coxon P, Downes CP, Smith SA, Macphee CH** 2001 Tumor suppressor and anti-inflammatory actions of PPARγ agonists are mediated via upregulation of PTEN. Curr Biol 11:764–768
55. **Frohlich E, Machicao F, Wahl R** 2005 Action of thiazolidinediones on differentiation, proliferation and apoptosis of normal and transformed thyrocytes in culture. Endocr Relat Cancer 12:291–303
56. **Park JW, Zarnegar R, Kanauchi H, Wong MG, Hyun WC, Ginzinger DG, Lobo M, Cotter P, Duh QY, Clark OH** 2005 Troglitazone, the peroxisome proliferator-activated receptor-γ agonist, induces antiproliferation and redifferentiation in human thyroid cancer cell lines. Thyroid 15:222–231
57. **Philips JC, Petite C, Willi JP, Buchegger F, Meier CA** 2004 Effect of peroxisome proliferator-activated receptor γ agonist, rosiglitazone, on dedifferentiated thyroid cancers. Nucl Med Commun 25:1183–1186
58. **Shiau CW, Yang CC, Kulp SK, Chen KF, Chen CS, Huang JW** 2005 Thiazolidenediones mediate apoptosis in prostate cancer cells in part through inhibition of Bcl-xL/Bcl-2 functions independently of PPARγ. Cancer Res 65:1561–1569
59. **Lu M, Kwan T, Yu C, Chen F, Freedman B, Schafer JM, Lee EJ, Jameson JL, Jordan VC, Cryns VL** 2005 Peroxisome proliferator-activated receptor γ agonists promote TRAIL-induced apoptosis by reducing survivin levels via cyclin D3 repression and cell cycle arrest. J Biol Chem 280:6742–6751
60. **Qi C, Zhu Y, Reddy JK** 2000 Peroxisome proliferator-activated receptors, coactivators, and downstream targets. Cell Biochem Biophys 32:187–204

Endocrinology **is published monthly by The Endocrine Society (http://www.endo-society.org), the foremost professional society serving the endocrine community.**